

A structural study of 2-*O*-lauroylsucrose with molecular modeling and NMR methods

Catherine Hervé du Penhoat ^a, Søren Balling Engelsen ^b,
Daniel Plusquellec ^c, Serge Pérez ^{d,*}

^a *Laboratoire de Chimie de l'Ecole Normale Supérieure, 24 rue Lhomond, 75231 Paris, France*

^b *The Royal Veterinary and Agricultural University, Department of Dairy and Food Science, Food Technology, Rolighedsvej 30, DK-1958 Frederiksberg C, Denmark*

^c *Laboratoire de Synthèses et Activations de Biomolécules, (associated with the CNRS), Ecole Nationale Supérieure de Chimie de Rennes, 35700 Rennes, France*

^d *Centre de Recherches sur les Macromolécules Végétales, CNRS, (associated with University Joseph Fourier), BP 53X, 38041 Grenoble Cédex, France*

Received 6 March 1997; accepted 15 August 1997

Abstract

The preferred conformations of sucrose, 2-*O*-acetylsucrose and 2-*O*-lauroylsucrose have been explored with the MM3 force field. The main effect of 2-*O*-substitution has been shown to be a slight decrease in accessible Φ , Ψ -space. The CICADA program, a heuristic searching algorithm, was used to investigate the favored conformers of 2-*O*-lauroylsucrose. The global minimum (Φ , Ψ = 73°, -81°) has been located in the A-well which contains the crystal structure of sucrose in the corresponding energy map. As this potential energy well is 2.9 kcal/mol below the other low-energy regions it represents the only conformational family which is expected to contribute significantly to the time-averaged properties. The other major conformational change with respect to sucrose concerns the CH₂-1f primary hydroxyl group which preferentially adopts the TG orientation instead of an equal distribution of rotamers in the case for sucrose. Restriction of the internal rotation of the CH₂-1f exocyclic results in distinct coupling constants between the HO-1f proton and the H-1Rf and H-1Sf spins and well-separated multiplets for the latter methylene protons. From the ¹³C relaxation data, it appears that the reorientation of the sucrosyl moiety is slightly anisotropic. A motional model similar to the one recently proposed for sucrose (internal motion of considerable amplitude, $S_{\text{ang}}^2 \sim 0.7$, occurring on the same timescale as overall tumbling) reproduced all the relaxation

Abbreviations: PES, potential energy surface

* Corresponding author. Tel.: +33-476-03-76-30; fax: +33-476-03-76-29; e-mail: perez@cermav.grenet.fr.

data. Finally, molecular modeling has shown that the favored position of the sidechain is an axial orientation with respect to the pyranose ring. © 1998 Elsevier Science Ltd

Keywords: 2-*O*-Lauroylsucrose; Molecular mechanics; Conformational search; NMR; Glycolipid; Molecular relaxation

1. Introduction

Amongst the numerous surfactants available, synthetic glycolipids are of the utmost importance for biological studies, e.g., extraction, purification and crystallization of membrane proteins [1]. 2-*O*-Lauroylsucrose (**1**) was initially synthesized for that purpose through a one-step procedure from unprotected sucrose [2]. Acylation of the 2-hydroxyl of sucrose makes the glycosidic bond much more resistant to enzymatic hydrolysis by invertase and the α -glucosidase from baker's yeast than that of the commercially available regioisomer 6-*O*-acylsucrose [3,4]. Owing to its extraction efficacy and its compatibility with protein structure and activity, 2-*O*-lauroylsucrose proved useful for the extraction of reticulum sarcoplasmic Ca^{+2} -ATPase, whereas its 10,11-dibromoundecanoyl analogue appeared an appropriate tool for investigating the topology of membrane proteins either in a biological membrane or in solubilized complexes [5]. In addition, the position of the alkyl chain gives this surfactant a particular umbrella shape. The effect of 2-*O*-lauroylsucrose on the physical properties of charged lamellar phases was therefore investigated in order to determine the role of glycoconjugates in biological membranes [6].

2-*O*-Lauroylsucrose has proven extremely difficult, if not impossible to organize in the form of single crystals. The molecule is a typical amphiphilic glycolipid with a hydrophilic sucrosyl moiety to which a hydrophobic acyl chain is attached. Usually such molecules tend to crystallize in a bilayer type of arrangement but apparently this molecule has great difficulty in occupying all the empty space in the crystal lattice with its acyl chain in the usual all-trans conformation. Simultaneous molecular modeling of 2-*O*-acetylsucrose (**2**) and 2-*O*-lauroylsucrose (**1**) was undertaken to determine the influence of the functional group and the aliphatic sidechain, respectively, on the conformation of the sucrosyl moiety. In parallel, an NMR study of 2-*O*-lauroylsaccharose was initiated to obtain experimental validation of the theoretical structures.

Obvious questions to be answered were the following: (a) What is the effect of the change from the O-2g hydroxyl oxygen in sucrose to acetal oxygen in

2-*O*-lauroylsucrose upon the preferred conformations about the glycosidic linkage and the hydrogen-bonding pattern? (b) What is the favored solution conformation of the acyl chain? (c) How does the presence of the lauroyl side chain influence the sucrosyl conformation? (d) What is the most likely aggregate or packing phenomena of the favored solution structures? and (e) How do the theoretical conformational search ensembles (using the new motional model from the sucrose MD-study) compare to experimental time-averaged data such as homo- and hetero-nuclear NMR relaxation parameters?

2. Methods

Nomenclature.—A schematic representation of 2-*O*-lauroylsucrose (2-*O*-lauroyl- β -D-fructofuranosyl-(2 \rightarrow 1)- α -D-glucopyranoside) along with numbering and labeling of the heavy atoms is shown in Fig. 1. In this study we consider eight main conformational degrees of freedom. The conformation about the glycosidic linkage bonds are described by the following torsion angles:

$$\Phi = \text{O-5g-C-1g-O-1g-C-2f}$$

$$\Psi = \text{C-1g-O-1g-C-2f-O-5f.}$$

The orientations of the three hydroxymethyl groups are described by the torsional angles:

$$\omega_g = \text{O-5g-C-5g-C-6g-O-6g}$$

$$\chi_f = \text{O-5f-C-2f-C-1f-O-1f}$$

$$\omega_f = \text{O-5f-C-5f-C-6f-O-6f.}$$

The orientation of the fatty acid group linked to O-2g is defined by the three torsional angles:

$$\gamma_1 = \text{C-1g-C-2g-O-2g-C-21g}$$

$$\gamma_2 = \text{C-2g-O-2g-C-21g-C-22g}$$

$$\gamma_3 = \text{O-2g-C-21g-C-22g-C-23g}$$

The sign of the torsion angles is defined in agreement with the IUPAC-IUB Commission of Biochemical Nomenclature [7]. The orientation of all dihedrals is according to the definition given in Fig. 2.

NMR spectroscopy.—400.13 MHz ^1H and 100.6 MHz ^{13}C NMR spectra of a 64-mM sample of 2-*O*-

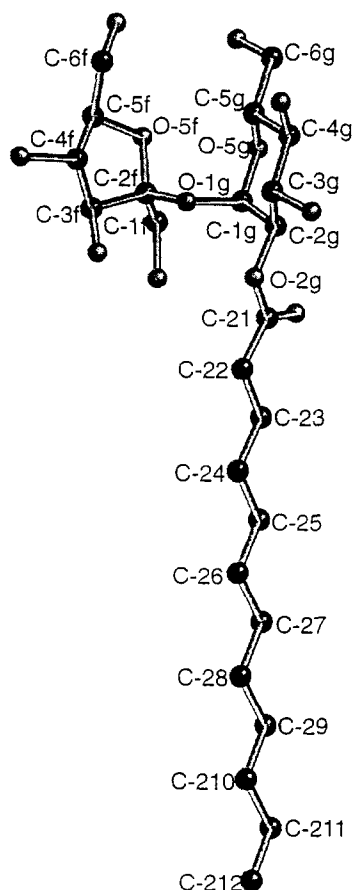


Fig. 1. Schematic representation of 2-*O*-lauroylsucrose (1) inclusive numbering and labeling of the heavy atoms.

lauroylsucrose in $\text{ME}_2\text{SO}-d_6$ were recorded on a Bruker DRX 400 operating in the Fourier transform mode at 294 K. Chemical shifts were assigned from 2D correlation spectra (COSY and HETCOR) and the vicinal proton coupling constants were extracted from a spectrum with a digital resolution of 0.5 Hz/pt. Vicinal heteronuclear coupling constants were obtained from selective INEPT2D spectra [8]. NOESY volumes and heteronuclear T_1 data were measured as previously described [9]. Heteronuclear NOE factors (η) were obtained by comparing fully-decoupled and inverse-gated carbon spectra.

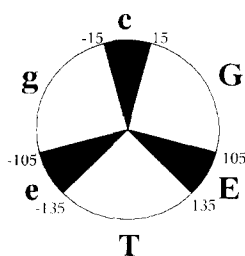


Fig. 2. Letter code for torsional angles.

Computational methods.—The conformational behavior of 2-*O*-lauroylsucrose was investigated using the MM3 force field (version 92) [10,11]. In addition to the classical terms the force field includes anisotropy of hydrogens, corrections for stereoelectronic effects, cross term effects like torsion–stretch, torsion–bend and bend–bend interactions. Buckingham type potential for non-bonded interactions and explicit terms for hydrogen bonding. No cut-off of nonbonded interactions was used and the dielectric constant was set to 4.0 [12].

Molecular mechanics grid search.—The potential energy surface of sucrose and 2-*O*-acetylsucrose was computed from 54 individual relaxed potential energy maps in vacuum. The starting conformation of the pyranosyl group was 4C_1 and the corresponding starting conformer for the furanosyl moiety was taken as the crystallographic 4T_3 conformation. For all 27 possible combinations of orientations (g/G/T) of ω_g , ω_f and χ_f a clockwise (c) and reverse clockwise (r) orientation of the secondary hydroxyl groups on the glucopyranosyl ring were considered, so as to best form a partial crown of intramolecular hydrogen bonds. Each of these conformations was fully optimized and used as a starting point for calculating a relaxed map. The relaxed maps were computed using rigid rotation followed by harmonic constraint minimization in 10° increments for Φ and Ψ spanning Φ in the range between 0° and 180° and the whole angular range of Ψ . Convergence was accepted when the iterative decrease in energy ΔE was less than $N \cdot 0.00008$ kcal/mol (where N was the number of atoms in the molecule). This approach resulted in 36,935 possible conformations from which a general adiabatic Φ , Ψ map was constructed by using the lowest energy values for the 54 relaxed maps.

Molecular mechanics CICADA search.—The CICADA program provides a conformational search shell for the underlying molecular mechanics program and it performs exploration of the potential energy surface, PES, of the molecule in dihedral space. The algorithm [13] has previously been applied to carbohydrates [14,15]. After completion, CICADA provides information about all conformations and transition states found in the search in standard coordinate files and in special geometry files containing energy and values of selected dihedral angles. For further advanced analysis CICADA provides a graph containing the accumulated information on interconversion pathways and transition states amongst the conformations.

The CICADA process is controlled by several

parameters of which the most important are the selected set of driven dihedrals, the identity criterion D_{\min} , the dihedral step increment $\Delta\Phi$, and the stop criterion E_{conf} . The identity criterion used to determine if two conformations are identical was set to 30° . The dihedral step increment was set to 20° with the result that we are not likely to observe much finer details in resulting transition states. This is not a regular grid increment as all local minima are fully relaxed. The stop criterion which was set to 10 kcal/mol is based on relative energy of conformations; if no more conformations are found in an energy window defined with respect to the global minimum then the algorithm will stop the search. Furthermore the efficiency of the CICADA process can be enhanced by enabling and disabling the individual dihedrals which are to be driven. In the initial search only the most important dihedrals (Φ , Ψ , ω_g , ω_f , χ_f , γ_1 , γ_2 and γ_3) were driven to avoid unnecessary time spent on rotating small side groups in regions of PES of insignificant importance. Then all hydroxyl groups were included in the search and finally all torsional angles of the acyl chain were driven.

Data simulation.—All simulated data were calculated using a Boltzmann distribution of complete molecular statics ensembles.

Coupling constants.—Coupling constants, $^3J_{\text{H,H}}$, for vicinal hydrogen atoms of a H–C–C–H segment were calculated using a Karplus type equation [16] with the Haasnoot–Altona parameterization [17]. It accounts for the J dependence on the dihedral angle of the H–C–C–H fragment, on the electronegativity of the participating atoms and on the orientation of the α and β substituents. The heteronuclear coupling constant $^3J_{\text{H,C}}$ across the glycosidic linkage was calculated by using the equation for the heteronuclear C–O–C–H segment proposed by Tvaroska et al. [18].

Rotamer distributions about primary hydroxyl groups were calculated numerically from the limiting values given by the Haasnoot–Altona equation [17,19]. All rotamer distributions were calculated using this set of equations. The results include negative populations arising from inaccuracies in the empirical Haasnoot–Altona description since only idealized staggered conformations are considered.

NMR relaxation data.—The relaxation data simulations take into account the geometric and dynamic aspects of conformational fluctuations through population-averaged distance matrices and a motional model, respectively. Homonuclear NMR relaxation

data were simulated with inhouse software [20] based on the model-free spectral densities [21]. In this approach, NOESY volumes were obtained by back-calculation of the relaxation matrix which was established from the CICADA ensemble distance matrices ($\langle r^{-6} \rangle$ and $\langle r^{-3} \rangle$). In one case, the distance matrix for a single structure was used to compute the NOESY volumes. Motional parameters (S_{ang}^2 , the spatial restriction of internal motion which is equal to 1 for a rigid molecule and to 0 for a totally flexible molecule; τ_e , correlation time of the internal motion; τ_c , correlation time of molecular reorientation or overall tumbling) were obtained by simultaneously fitting both the homo- and heteronuclear relaxation data.

3. Results and discussion

Adiabatic map.—The potential energy surface (PES) of sucrose in the MM3 force field is shown in Fig. 3a. The map has the characteristic shape of a small belt spanning almost the whole Ψ -space, roughly in the region $\Phi = 60^\circ$ to 120° ; it corresponds closely to previous published maps of sucrose in the MM3 force field [22,23].

The steric effects of a 2-*O*-substitution are illustrated in Fig. 3b, with the PES for 2-*O*-acetylsucrose. The main effect of the 2-*O*-acetyl substitution is a slightly more restricted PES. The lowest energy minimum occurs at Φ , $\Psi = 70^\circ$, -80° which is shifted by -37° and -35° from the crystalline sucrose conformation. Within 8 kcal/mol the occupied area in (Φ, Ψ) -space of the 2-*O*-acetylsucrose adiabatic map is 21% and the calculated 3D volume is $138 \times 10^3 \text{ deg}^2 \text{ kcal/mol}$. In comparison, occupied area in (Φ, Ψ) -space of the sucrose adiabatic map is 23% and the calculated 3D volume is $151 \times 10^3 \text{ deg}^2 \text{ kcal/mol}$.

CICADA search.—Fig. 4a shows all 1293 (all-trans) conformations of 2-*O*-lauroylsucrose found by the CICADA search, superimposed on the adiabatic map of 2-*O*-acetylsucrose. The conformations cluster in four main areas: in the center of the A-well, along a line in the center of the B-well, in the center of the C-well and in the upper part (AX) of the A-well where the crystal conformation of sucrose is found. The fact that the AX area is not a local minimum on the 2-*O*-acetylsucrose adiabatic map does not exclude that individual maps have local minima in this area. The corresponding plot of the 2-*O*-lauroylsucrose transition states in Fig. 4b reveals interesting features.

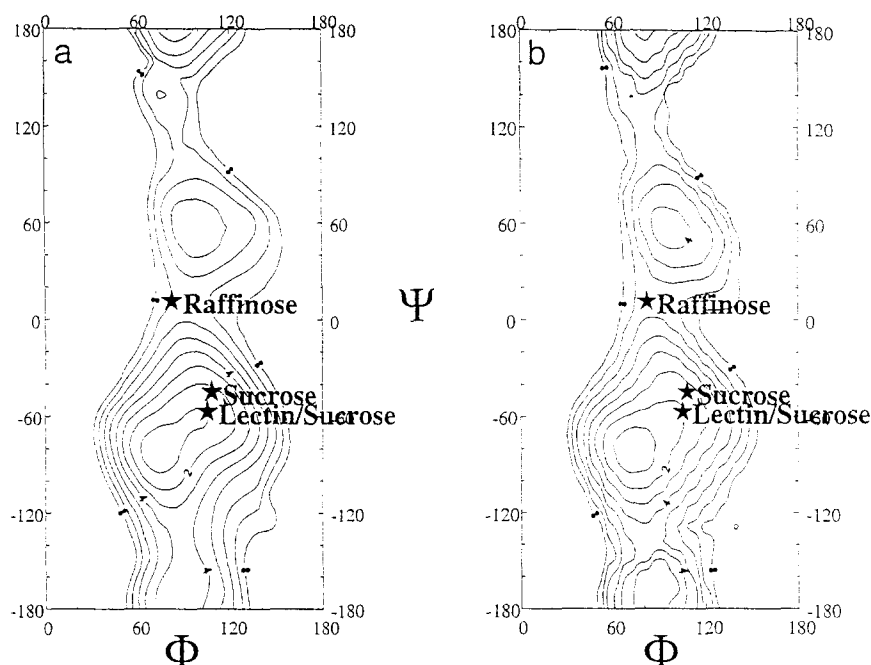


Fig. 3. (a) Adiabatic map of sucrose (S.B. Engelsen, Unpublished data). (b) Adiabatic map of 2-*O*-acetylsucrose (**2**) in the MM3 force field with indications of the positions of crystallographic conformations of sucrose (★) including the crystal structure of sucrose [24], the crystal structure of raffinose and the crystal structure of a hydrated sucrose found in a lentil lectin [27]. Isoenergy contours are drawn in 1 kcal/mol intervals up to 8 kcal/mol from the global minimum.

As to be expected most transition states are located in saddle point regions but also a large number of transition states are found in the center of the A- and

B-wells corresponding to local (non Φ, Ψ -space) conformational interconversion pathways. The total absence of transition states in the C-well indicates a flat

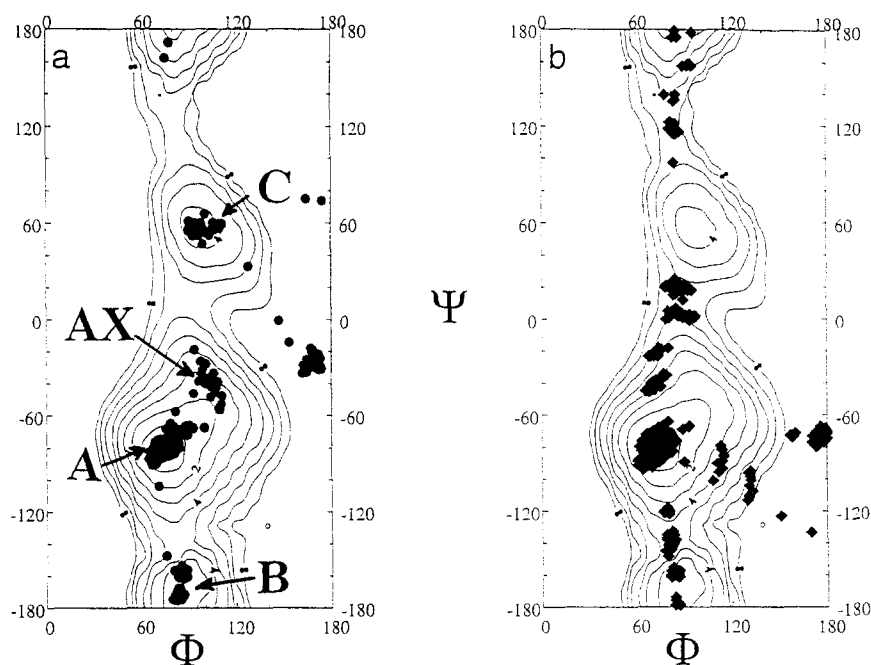


Fig. 4. (a) CICADA conformations and (b) transition states superimposed on the 2-*O*-acetylsucrose adiabatic map. Isoenergy contours are drawn in 1 kcal/mol intervals up to 8 kcal/mol.

Table 1

List of conformations of 2-*O*-lauroylsucrose found by the CICADA search

Well/rating ^a	Φ_1	Ψ_1	Suc ^b	Lauroyl ^c	Acyl chain	ΔE^d	p_i^e
A1*	73	−82	GTG	GTT	ggTTGTTTT	−1.4022	
A1	73	−81	GTG	GTc	TTTTTTTTT	0.0000	7.1485
A2	73	−81	GTG	GTg	TTTTTTTTT	0.1018	6.0055
A3	74	−80	GTG	GTc	TTTTTTTTT	0.3424	3.9785
A4	76	−80	GTG	GTg	TTTTTTTTT	0.4326	3.4094
A5	71	−81	GGG	GTG	TTTTTTTTT	0.8913	1.5551
A6	72	−81	GGG	GTg	TTTTTTTTT	0.9206	1.4790
A7	72	−80	GGG	GTG	TTTTTTTTT	1.1120	1.0659
A8	72	−81	GGG	GTG	TTTTTTTTT	1.1416	1.0132
A9	73	−81	GGG	GTG	TTTTTTTTT	1.1429	1.0110
AX155	109	−56	GTG	GTg	TTTTTTTTT	2.3613	0.1257
B280	84	−158	GTG	GTg	TTTTTTTTT	2.8752	0.0521
C621	93	59	GTG	GTc	TTTTTTTTT	3.8065	0.0106

Conformations contributing more than 1% to the total population are listed in descending order together with the two local minima from the B- and C-wells. Populations are based on all-trans conformers, but for comparison the A1* conformation is included which was the lowest energy conformer found when the acyl chain was also driven.

^a Throughout the paper conformers will be referred to using the uppercase letter indicating the local well and the global energy rating in the all-trans CICADA search (the asterisk indicates the total search which encompass also cis-conformers of the acyl chain).

^b Primary hydroxyl group dihedrals of the sucrose moiety: ω_g , χ_f and ω_f . Letter code is written according to Fig. 2.

^c The conformation of the lauroyl moiety: γ_1 , γ_2 and γ_3 . Letter code is written according to Fig. 2.

^d Relative energy in kcal/mol calculated with respect to the global minimum.

^e Population of conformer in per cent (298 K).

local minimum region governed by steric restrictions in Φ , Ψ -space with a very low conformational diversity.

In Table 1 some of the most populated conformations of 2-*O*-lauroylsucrose with the acyl chain in the all-trans conformation are listed. The global A-well minimum is 2.9 kcal/mol below the local B-well minimum and 3.8 kcal/mol below the local C-well minimum. Taking into account the lower conformational diversity of these wells, it is clear that B- and C-well conformations will not contribute significantly to any calculated observables (at 300 K) or to any properties which reflect the Boltzmann distribution. The local minimum of the AX part of the A-well is

slightly lower in energy than the corresponding B-well minimum and considering the higher conformational diversity of this region, AX-conformations are likely to contribute significantly to calculated properties. The lauroyl moiety was also driven in the final part of the conformational search and the global minimum was 1.4 kcal/mol lower in energy than the global minimum of the all-trans search. This energy difference stems from an optimization of the non-bonded interactions between the sucrosyl and lauroyl moieties in the vacuum simulations.

Intramolecular hydrogen bonds.—The crystal structure of sucrose possesses two strong intramolecular hydrogen bonds: HO-2g \cdots O-1f and O-

Table 2

Intramolecular oxygen–oxygen distances and radius of gyration of selected conformers of 2-*O*-lauroylsucrose

Well/rating	O-2g \cdots O-1f	O-2g \cdots O-3f	O-5g \cdots O-6f	O-6g \cdots O-6f	R_g
Sucrose	2.78	4.84	2.85	4.01	3.17
Lectin/sucrose	4.9	4.5	4.5	5.5	3.2
A1*	4.083	3.963	4.749	3.005	4.299
A1	4.067	4.037	4.703	2.977	5.597
A2	4.033	3.986	4.680	2.949	5.906
AX155	3.307	4.571	4.673	4.485	5.768
B280	5.042	3.525	6.294	6.731	5.767
C621	5.319	5.436	6.024	8.227	5.635

5g \cdots HO-6f [24]. Recent X-ray, NMR and modeling studies strongly indicate that both of these hydrogen bonds are broken (very lowly-populated) in dilute aqueous solution [9,23]. Instead two relatively highly-populated bridging water situations, O-2g \cdots Ow \cdots O-1f and O-2g \cdots Ow \cdots O-3f, have been proposed from modeling studies [9,25,26] and the latter one is observed in a hydrated crystal structure embedded in a lentil lectin crystal [27]. In this perspective 2-*O*-lauroylsucrose is a quite interesting structure as the O-2g atom is changed from a hydroxyl oxygen (in sucrose) with both accepting and donating capabilities to an accepting only acyl oxygen. Furthermore the hydrogen bonding capabilities of the O-2g acyl oxygen is expected to be less competitive and less exposed due to the neighboring carbonyl group. It is therefore to be expected that the influence of the O-2g atom which is a key atom in determining the sucrosyl conformation of sucrose (and raffinose) will be less important in the case of 2-*O*-acyl derivatives. Table 2 lists the distances for all possible intraring hydrogen bonds of the most important conformers of 2-*O*-lauroylsucrose. In contrast to similar in vacuo studies on sucrose [9,23] none of the minimum energy conformers possess intraring hydrogen bonds, except for A1 and A2 (and A1*) which both have a stabilizing hydrogen bond between the two C-6 primary hydroxyl groups. However, such intramolecular hydrogen bonds between two flexible side groups are not likely to be able to compete on a statistical basis with water interactions. From the relatively short distance, it might appear that a weak electrostatic interaction exists in one conformer (AX155) between the O-2g and O-1f groups but, in fact, the HO-1f points in another direction. Although the carbonyl oxygen is expected to be an important factor in intermolecular interactions no conformer has been found in which this group forms intramolecular hydrogen bonds, primarily due to its strong tendency to align parallel with the C-2g–H-2g bond. This is indicated in Fig. 5g where the cis conformations of γ_2 are not found within a 10 kcal/mol window.

The glycosidic linkage.—The fact that the 2-*O* substitution diminishes the hydrogen bonding capabilities of the sucrosyl moiety is expected to have some influence on the conformations about the glycosidic linkage. In the case of sucrose, the $^3J_{\text{H,C}}$ parameters are only calculated correctly if explicit water molecules are included in the simulations [9]. This is because this conformational equilibrium is dominated by sucrose conformations with a stabilizing water

molecule bridging O-2g and either O-1f or O-3f. In these vacuum calculations, we did not find any significant influence of the 2-*O*-acylation upon the conformational equilibrium; this is revealed by the simulations as the conformational preference (g/G/T) of Ψ at 300 K remains unchanged (99:0:1) when compared to sucrose (see also Fig. 5b). These results are corroborated experimentally by identical values of $^3J_{\text{H-1g,C-2f}}$ for **1** and sucrose (Table 3).

The ring conformations.—The theoretical glucosyl vicinal ring couplings are in a good agreement with the experimental ones which is consistent with the preservation of the 4C_1 chair conformation of the glucose residue throughout the simulation. However, the small shifts in experimental vicinal ring couplings from sucrose to 2-*O*-lauroylsucrose are not reflected in the modeling. Also the more flexible furanosyl ring remained in its northern conformation throughout the CICADA search which is weakly supported by the NMR data.

Primary hydroxyl rotamer populations.—The rotamer distribution around the ω_g primary hydroxyl group (Fig. 5c) calculated from the CICADA ensemble results in a g/G/T ratio of 10:88:2 (300 K) which is similar to the ratio calculated for sucrose: 7:91:2. However, both ratios favor the G rotamer with respect to the g rotamer more than is to be expected from the NMR coupling constant data which indicates an approximate 50:50:0 ratio [19]. Also the ω_f rotamer distribution of 3:96:1 (Fig. 5d) is calculated to be similar to that of sucrose (5:92:3) indicating that the 2-*O*-substitution has no conformational effects on the relatively remote C-6g and C-6f hydroxyl groups.

As would be expected, the conformational preference of the C-1f primary hydroxyl group, which is in close proximity to the 2-*O*-acyl group, is different from that of sucrose. While the C-1f rotamer distribution in sucrose is found to have a relatively equal distribution, the corresponding distribution in 2-*O*-lauroylsucrose (Fig. 5e) is calculated to be more in favor of the *T* conformation: 12:12:76.

Acyl chain orientation.—The orientation of the all-trans acyl chain with respect to the sucrosyl moiety is assessed by the three torsional angles γ_1 , γ_2 and γ_3 (Fig. 5f–h). Due to a beneficial local interaction between the C-2g–H-2g bond and the carbonyl C=O bond, the γ_1 and especially γ_2 rotamers are kept relatively fixed in their G and T conformations, respectively. γ_3 displays an interesting feature: the global all-trans minimum is found to have γ_3 in the cis conformation with an angle of 13°. The effect of

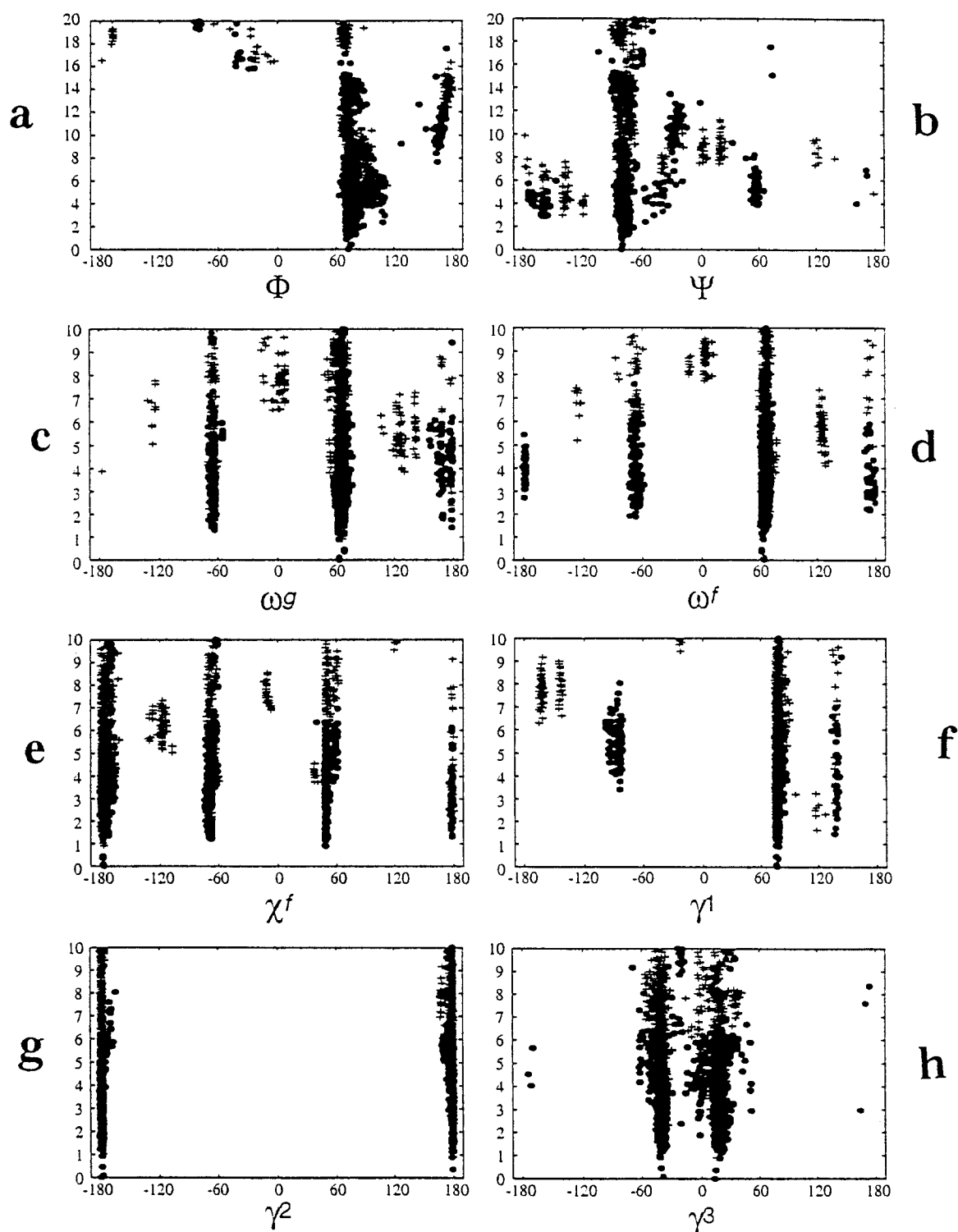


Fig. 5. One-dimensional plots of important dihedral angles versus energy of conformations (●) of 2-*O*-lauroylsucrose found by the CICADA search: (a) Φ , (b) Ψ , (c) ω_g , (d) χ_f , (e) ω_f , (f) γ_1 , (g) γ_2 and (h) γ_3 .

the cis orientation of γ_3 is a relatively axial orientation of the acyl chain with respect to the pyranose ring in contrast to the staggered g, G and T conformers which promote more elongated equatorial type

orientations of the acyl chain. The less elongated form of the cis structure is also reflected by the radius of gyration (Table 2) which is 5.6 Å in comparison to 5.9 Å for the g structure. The stabilization

Table 3

Observed and calculated 3J coupling constants (Hz) for 2-*O*-lauroylsucrose compared with those of sucrose

3J	2- <i>O</i> -Lauroylsucrose Experimental	Calcd ^a	Calcd ^b	Sucrose Experimental ^c	Calcd ^e
<i>α-Glcp</i>					
H-1g, H-2g	3.8	3.7	3.6	3.8	3.7
H-2g, H-3g	10.3	9.5	9.6	10.0	9.6
H-3g, H-4g	9.6	9.3	9.3	9.1	9.3
H-4g, H-5g	9.4	9.8	9.8	9.8	9.8
H-5g, H-6sg	1.9	1.0	1.4	2.0	2.6
H-5g, H-6rg	5.6	10.5	9.9	5.0	9.6
g/G/T		10:88:2	3:96:1		7:91:2
<i>β-Fruf</i>					
H-3f, H-4f	8.5	8.8	8.8	8.8	8.8
H-4f, H-5f	—	9.0	9.1	8.3	9.0
H-5f, H-6sf	—	10.7	10.4	7.1	10.2
H-5f, H-6rf	—	1.0	1.1	3.7	1.4
g/G/T		3:96:1	1:99:0		5:92:3
<i>α(1 → 2)</i>					
H-1g, C-2f	3.8	2.6	2.8	3.8 ^d	2.7

^a Calculated from the complete theoretical ensemble.^b Calculated from the theoretical ensemble with the acyl chain in its all-trans configuration.^c From ref. [9].^d Experimental value obtained in the course of the present study.^e Calculated from the theoretical ensemble from ref. [23].

Table 4

100.6 MHz ^{13}C NMR data of a 64 mM solution of the 2-*O*-lauroylsucrose in $\text{Me}_2\text{SO}-d_6$ (δ_{Me} 39.5 ppm)

Carbon	δ (ppm)	T_1 (s) (average deviation)	Heteronuclear Overhauser effect η (average deviation)
<i>α-Glcp</i>			
C-1g	88.73	0.22 (0.00)	0.81 (0.03)
C-2g	73.10	0.22 (0.00)	0.82 ⁵ (0.015)
C-3g	69.82	0.23 (0.00)	0.87 ⁵ (0.005)
C-4g	70.01	0.23 ⁵ (0.005)	0.87 ⁵ (0.005)
C-5g	72.62	0.23 (0.00)	0.88 (0.00)
C-6g	60.28	0.14 (0.00)	1.00 (0.00)
<i>β-Fruf</i>			
C-1f	61.02	0.13 ⁵ (0.005)	1.01 (0.05)
C-2f	104.29 ^a	na	na
C-3f	75.20	0.23 (0.005)	0.75 (0.04)
C-4f	73.75	0.23 (0.00)	0.77 (0.02)
C-5f	82.74	0.23 (0.00)	0.84 (0.003)
C-6f	62.36	0.16 ⁵ (0.005)	0.91 (0.03)
<i>Lauroyl sidechain</i>			
C-21''	172.97	na	na
C-22''	33.60	0.26 (0.00)	1.13 (0.04)
C-23''	31.37	na	na
C-24''–C-29''	29 (br m)	na	na
C-210''	24.28	0.36 (0.00)	1.14 (0.04)
C-211''	22.17	na	na
C-212''	14.03	na	na

na = Not applicable or not accessible.

⁵ $J_{\text{H}-1,\text{C}-2}$ 3.8 Hz.

Table 5
400.13 MHz ^1H NMR data^a of a 64 mM solution of the 2-*O*-lauroylsucrose in $\text{Me}_2\text{SO}-d_6$ (δ_{Me} 2.72 ppm)

Proton	δ (ppm)	Multiplicity	$^3J_{\text{A},\text{A}+1}$ or $^2J_{\text{AS},\text{AR}}$
<i>α-Glcp</i>			
H-1g	5.515	d	3.8
H-2g	4.585	dd	10.3
H-3g	3.869	\sim t	9.6
H-4g	3.44	\sim t	9.4
H-5g	3.91	m	
H-6Sg	3.81 ^b	dd	−11.3, 1.9
H-6Rg	3.72 ^b	dd	−11.3, 5.6
HO-3g ^c	5.258	d	5.4
HO-4g ^c	5.213	d	5.9
HO-6g ^c	4.572	t	5.4
<i>β-Fru_f</i>			
H-1Sf	3.500	AB	−11.3
H-1Rf	3.328	AB	−11.3
H-3f	4.190	d	8.5
H-4f	3.96	\sim t	
H-5f	3.77	m	
CH ₂ -6f	3.77	m	
HO-1f ^c	5.076	dd	7.3 (H-1Sf) 4.9 (H-1Rf)
HO-3f ^c	4.925	d	7.3
HO-4f ^c	5.394	d	5.9
HO-6f ^c	4.718	\sim t	5.4
<i>Lauroyl sidechain</i>			
CH ₂ -22''	2.512	ABXX'	
CH ₂ -23''	1.738	m	
CH ₂ -24''–CH ₂ -21''	1.459	m	
CH ₃ -212''	1.070	\sim t	\sim 6.8

^a Multiplicity of the aliphatic protons corresponds to an exchange-broadened spectrum acquired a week after sample preparation.

Key: d, doublet; t, triplet; m, multiplet.

^b ν_{AB} , 3.768 ppm.

^c Measured immediately upon preparation of the sealed NMR tube.

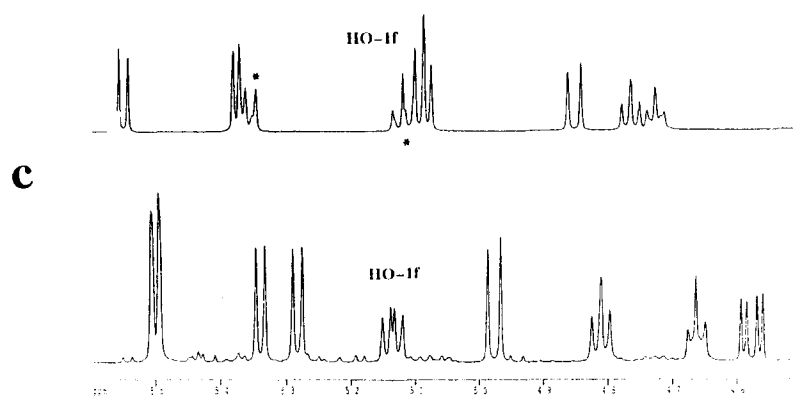
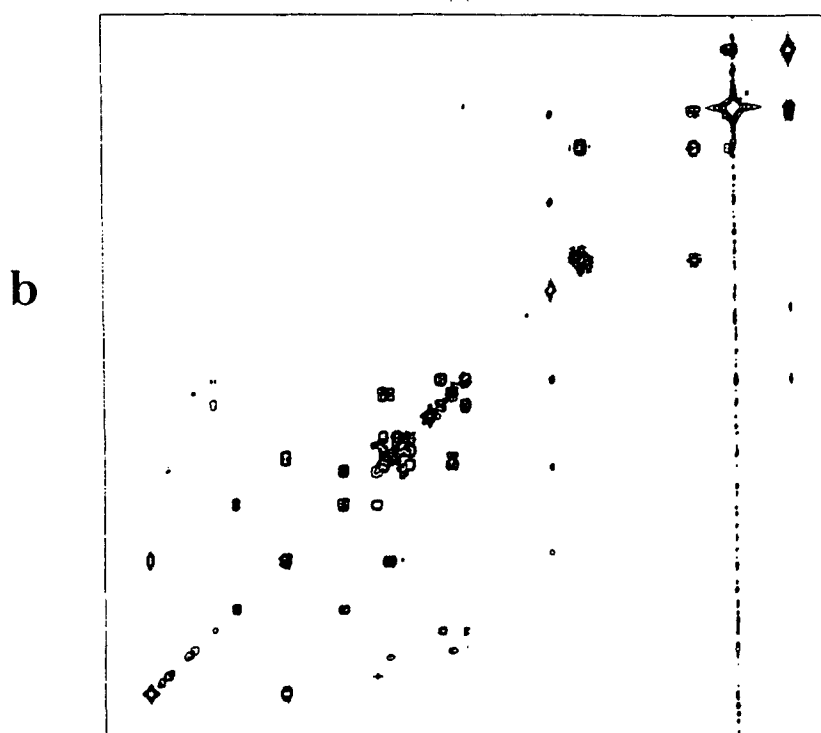
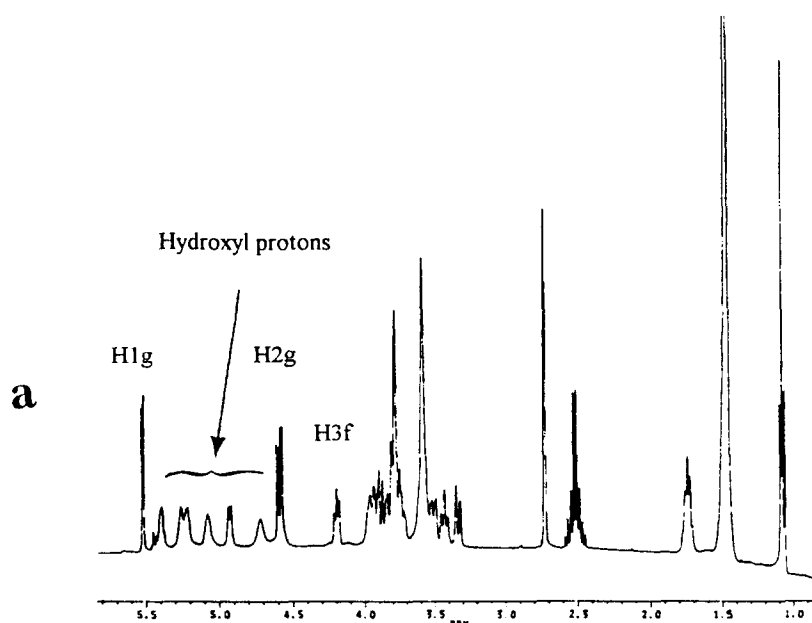
of the *cis* conformation of γ_3 is provided by weak favorable interactions between the C-23 methylene hydrogens and the O-2g ester oxygen (approximate distance of 2.6 Å). The global minimum is only about 0.1 kcal/mol below the global minimum having the γ_3 in its *g* conformation (Table 1).

NMR Spectroscopy.—*Chemical shift assignments and coupling constant data.* The carbon and proton chemical shifts of 2-*O*-lauroylsucrose, in $\text{Me}_2\text{SO}-d_6$,

were assigned from 2D correlation spectra (COSY and HETCOR) and these data have been collected in Tables 4 and 5, respectively. Comparison of these data with those described for sucrose in $\text{Me}_2\text{SO}-d_6$ [28] showed that the expected downfield shifts of the C-2 and H-2 resonances upon substitution by an acyl group [29] were observed for 2-*O*-lauroylsucrose along with upfield shifts (\sim 2–3 ppm) of the β -carbons. Secondary isotope multiplets [30,31] due to β (0.09–0.12 ppm) and γ (< 0.07 ppm) upfield deuterium isotope effects were detected in the carbon spectra of 2-*O*-lauroylsucrose in mixtures of $\text{Me}_2\text{SO}-d_6$ and deuterium oxide confirming the chemical shift assignments. A major difference was observed in the fine structure of the H-1fa and H-1fb signals which are best described as a tightly-coupled $\sim A_2$ pattern in the case of sucrose and a weakly-coupled AB system ($\Delta\nu = 69$ Hz) for 2-*O*-lauroylsucrose (where H-1fa and H-1fb correspond to the methylene protons whose signals resonate at low and high field, respectively).

Vicinal coupling constants were detected for the hydroxyl resonances of 2-*O*-lauroylsucrose in freshly-dissolved samples in $\text{Me}_2\text{SO}-d_6$ and these parameters are given in Table 5. The hydroxyl proton regions in the 400.13 MHz spectra of both 2-*O*-lauroylsucrose (below) and sucrose (above) are shown in Fig. 6. In order to dissolve the sucrose sample a drop of deuterium oxide was added and the multiplet pattern shows the same deuterium isotope effects as reported earlier [32]. The two hydroxyl coupling constants of the HO-1f group of 2-*O*-lauroylsucrose (7.3 and 4.9 Hz for $^3J_{\text{HO,H-1fa}}$ and $^3J_{\text{HO,H-1fb}}$, respectively) are distinctly different whereas a unique coupling constant (triplet, 5.4 Hz) was detected for the HO-1f moiety in the case of sucrose. Both the $^3J_{\text{H-1f,OH}}$ coupling constants and the fairly well-resolved AB system of the CH₂-1f methylene protons suggest that the time-averaged orientation of the H–O–C-1f–H-1Rf and H–O–C-1f–H-1Sf dihedrals of 2-*O*-lauroylsucrose are very different and would tend to indicate that rotation of the HOCH₂-1f hydroxymethyl group of 2-*O*-lauroylsucrose is much more spatially-restricted than in the case of sucrose. The asymmetrical triplet observed for HO-6f (4.67 ppm)

Fig. 6. (a) 400.13 MHz ^1H spectrum of 2-*O*-lauroyl sucrose in $\text{Me}_2\text{SO}-d_6$. (b) ^1H COSY spectrum. (c) The region containing the hydroxyl resonances in the 400.13 MHz NMR spectra of solutions (\sim 50 mM) of 2-*O*-lauroylsucrose (below) and sucrose (above; a drop of deuterium oxide was added) in $\text{Me}_2\text{SO}-d_6$. The multiplets of the HO-1f hydroxyl resonances have been labeled and deuterium isotope effects in the sucrose spectrum have been marked with an asterisk (*).



reflects second order effects due to the tightly-coupled ABCX system (H-6fa, H-6fb, H-5f and HO-6f). The sample used for the NMR study contained small (< 10%) amounts of related compounds which were the result of scrambling of the ester group with respect to various hydroxyl moieties (Fig. 6).

Acyl migrations under acid- and base-catalyzed conditions are frequently observed in partially acylated carbohydrates and have been a subject of numerous reports [33,34]. We have effectively shown that isomerization of 2-*O*-lauroylsucrose occurred intramolecularly to provide the 3-*O*- and then the 6-*O*-lauroyl regioisomers [35]. Nevertheless, strongly basic conditions, i.e., a nucleophilic base in Me₂NCHO or an aqueous solution of triethylamine were required [2]. Under the conditions used here, 2-*O*-lauroylsucrose was stable over a period of several weeks in Me₂SO-*d*₆ whereas some acyl migration (< 10%) was observed over the same period in deuterium oxide.

The hydroxyl signals broadened rapidly and no splitting was detected in the spectra used to measure the coupling constants of the methine and methylene protons. All of the ³*J*_{H,H} values of the glucosyl ring protons could be determined and these data, which are almost identical to those reported for sucrose, indicate the classical ⁴C₁ chair form of the pyranose ring. The experimental values of 5.6 and 2 Hz for the ³*J*_{H-5g,H-6gR} and ³*J*_{H-5g,H-6gS} coupling constants of 2-*O*-lauroylsucrose are also analogous to those of sucrose (4.5 and 2 Hz, ref. [28]). In a conformational study of hydroxymethyl groups in carbohydrates based on NMR data, Bock and Duus [19] have interpreted similar results obtained for various glucose derivatives in terms of an ~ 1:1 mixture of *g* and *G* rotamers.

The spectral dispersion of the fructosyl protons was unfavorable and only the ³*J*_{H-3f,H-4f} value could be precisely measured. According to the crosspeak pattern of the NOESY spectrum, the fine structure of the H-4f multiplet was close to being a triplet. The H-5f, H-6Rf and H-6Sf spins all resonated near 3.7 ppm forming a tightly-coupled system that was not amenable to analysis. The partial coupling data of the five-membered ring pointed to the ⁴*T*₃ puckering family located in the northern half of the pseudorotation wheel. The 3.8-Hz value of the ³*J*_{H-1g,C-2f} coupling constant of 2-*O*-lauroylsucrose was identical to the one reported for sucrose in Me₂SO-*d*₆ (this work) indicating a similar time-averaged orientation about the glycosidic linkage.

Carbon relaxation data.—In dilute solution, local fluctuating magnetic fields arise due to the random motion of neighbouring magnetic dipoles within the same molecule. These local fields can induce transitions in nuclear spin state thus modulating the return to equilibrium (or spin relaxation) in NMR experiments. In the case of small carbohydrates, both proton and carbon spin relaxation are dominated by this dipole–dipole mechanism. Molecular motion with a rate at the reciprocal of the NMR transition frequency (nanosecond timescale) will be the most efficient at bringing about relaxation and both overall tumbling (rotational diffusion) and internal motions of small carbohydrates fall within this category. Simulation of relaxation data therefore requires a description of molecular dynamics which must be accounted for with appropriate spectral densities. A motional model is most often obtained from heteronuclear relaxation data where the relaxation parameters can be expressed in terms of interactions with directly-attached protons. For instance, the carbon-proton distance can be assimilated to a fixed distance (1.11 Å) and the relaxation parameters can be fitted to various motional models in order to determine the nature of overall tumbling and the extent of internal dynamics. Accordingly, the average values of the experimental carbon longitudinal relaxation times, *T*₁, and NOE factors, *η*, (average deviations are given in brackets) were established and these data are collected in Table 4.

Molecular rotational diffusion.—In an investigation of sucrose in Me₂SO-*d*₆ [37], two groups of spins were distinguished on the basis of small differences in carbon *T*₁ values (5%) and slightly anisotropic reorientation was postulated. It was argued that the orientation of C–H vectors associated with the longer *T*₁s (2g, 3g, 4g, and 5g) was perpendicular to the long axis whereas the orientation of C–H vectors associated with the shorter *T*₁s (1g, 3f, 4f, and 5f) was almost parallel to this same axis. The presence of the 2-*O*-lauroyl sidechain would be expected to lead to even greater anisotropy in molecular reorientation. Indeed, hydrocarbon chains attached to fluorene have been shown to induce anisotropic reorientation which resulted in very large variations in the *T*₁ values (0.47–1.00 s) of the aromatic carbons depending on the orientation of the corresponding C–H vectors of the anchor [36].

This tendency was not evident in the case of 2-*O*-lauroylsucrose as the *T*₁ values of the methine carbons were almost identical (0.23 ± 0.005 s) and

would be compatible with isotropic overall tumbling [38]. In contrast, inspection of the η parameter of the 2-*O*-lauroylsucrose methine carbons reveals a considerable spread in values (0.75 to 0.88). In the case of isotropic tumbling, it has been shown [39] that internal motion of sufficient amplitude (order parameter < 0.8) can strongly modulate (100%) η values when this motion is relatively slow (correlation time > 0.05 ns). However, this implies notable differences in either the amplitude or in the timescales of the internal motion at the various methine carbons which seemed unlikely. In order to understand the influence of anisotropic tumbling on the carbon relaxation parameters of 2-*O*-lauroylsucrose, these data were simulated for axially-symmetric anisotropic tumbling [40,41] in the presence of internal motion [21].

The motional and geometric parameters for axially-symmetric anisotropic tumbling [21,40,41] include correlation times for rotation about the long (τ_{\parallel}) and short (τ_{\perp}) molecular axes and for internal motion (τ_i), the amplitude of internal motion (S_{ang}^2) and the angle (θ) between the C–H vector and the long axis. Variations in the T_1 and η values as a function of θ have been plotted in Fig. 7a and b, respectively, for the preferred motional model (vide infra). Almost no change (< 0.01 s) in the T_1 value is observed when the orientation of the C–H vector is varied over the whole angular range. However, the η value increases from 0.75 ($\theta = 0, 180$) to 0.90 ($\theta = 90, 270$). Inspection of a favored conformer of (1), the AX155 structure, shows that the C-2g, C-3g, C-4g, and C-5g methine carbons of the glucosyl residue are aligned perpendicular to the plane of the six-membered ring while C-1g, C-3f, C-4f, and C-5f are orientated nearly parallel to this plane. Thus the methine carbon relaxation data of 2-*O*-lauroylsucrose could be satisfactorily simulated by slightly anisotropic tumbling (anisotropic ratio of 1.6–1.7).

Internal motion.—As has been reported for sucrose [9], a continuum of motional models reproduces the carbon relaxation of 2-*O*-lauroylsucrose (S_{ang}^2 0.9 \rightarrow 0.7 with simultaneous variations in the correlation times, τ_{\perp} 0.65 \rightarrow 0.80, τ_{\parallel} 0.38 \rightarrow 0.50 and τ_i 0.01 \rightarrow 0.1 ns). In the former study [9], calculations of the amplitude of internal motion from a nanosecond-MD simulation in explicit water indicated that S_{ang}^2 values of 0.7 were the most appropriate and therefore the corresponding anisotropic motional model was adopted in the case of 2-*O*-lauroylsucrose ($S_{\text{ang}}^2 = 0.7$; τ_{\perp} , τ_{\parallel} , and τ_i values of 0.80, 0.50, and 0.1 ns respectively). It has been shown that when the anisotropic ratio ($\tau_{\perp}/\tau_{\parallel}$) is small (< 2), it does not

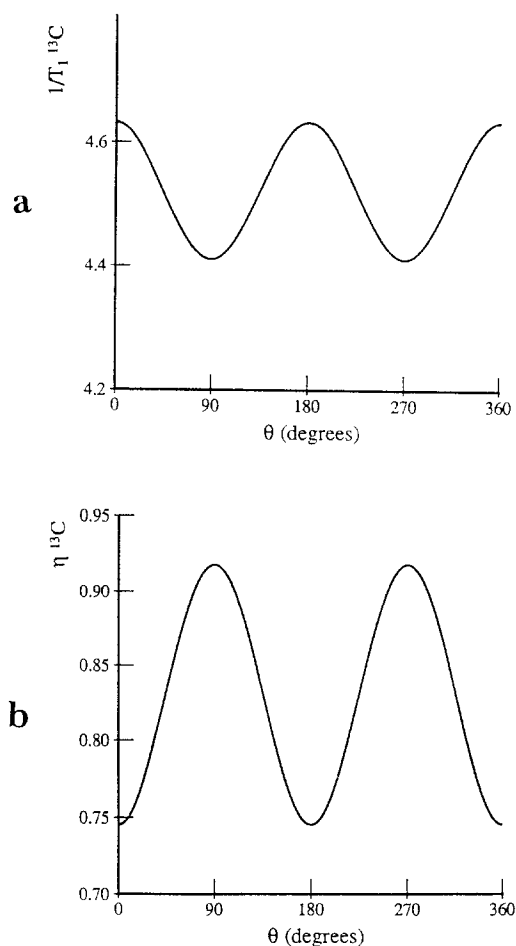


Fig. 7. (a) Theoretical plots of 100.6 MHz carbon longitudinal relaxation rates (T_1^{-1} , s^{-1}) as a function of the angle, θ (in degrees), between the C–H vector and the principal molecular axis established for anisotropic axially symmetric overall tumbling using the model-free spectral densities and the following motional model: ($S_{\text{ang}}^2 = 0.7$; τ_{\perp} , τ_{\parallel} , and τ_i values of 0.80, 0.50, and 0.1 ns respectively). (b) Theoretical plots of 100.6 MHz carbon nuclear Overhauser effects (η , s^{-1}) as a function of the angle, θ (in degrees), between the C–H vector and the principal molecular axis established for anisotropic axially symmetric overall using the model-free spectral densities and the motional model in (a).

significantly influence homonuclear relaxation data [42] so that the proton relaxation data were simulated with spectral densities appropriate for isotropic tumbling and motional parameters closely-related to those described above ($S_{\text{ang}}^2 = 0.7$; τ_c and τ_i values of 0.7 and 0.1 ns, respectively).

The relative flexibility of the various methylene protons could be estimated by comparison of the corresponding NT_1 values which are expected to be close to the average T_1 value of the methine protons in the absence of internal motion and much higher in

the case of rapid dynamics. Based on this criterion, it could be inferred that the motion of the pendant groups increases in the following order, C-1f < C-6g < C-6f < C-22 < C-23 to C-212.

Proton relaxation data.—The phase-sensitive NOESY spectrum of 2-*O*-lauroylsucrose acquired with a 1-s mixing time contained weak positive crosspeaks between sugar protons indicating that 2-*O*-lauroylsucrose was in the negative NOE regime. At 400.13 MHz, this implies that the τ_c value must be greater than 0.44 ns (zero-crossing at which the NOEs become gradually smaller). Broad crosspeaks were observed between the residual water protons and the methylene and methine protons. The latter peaks are the result of indirect transfer pathways (CH \rightarrow OH \rightarrow H₂O) as no crosspeaks are detected between hydroxyl protons and the other sugar protons. The corresponding normalized NOESY diagonal and crosspeak volumes are collected in Table 6.

Table 6
Experimental^a and theoretical 400.13 MHz normalized NOESY volumes of a 64 mM solution of the 2-*O*-lauroylsucrose in Me₂SO-*d*₆ acquired with a 1-s mixing time

	H-1g	H-2g	H-4g	H-1fb	H-3f	H-4f	Other
H-1g	0.301 ^a	0.017 ^a		0.005 ^a			
	0.221	0.017		0.008			
	0.274	0.016		0.013			
H-2g		0.362 ^a	0.019 ^a				0.007 ^a (H ₂ O)
		0.410	0.013				0.007
		0.420	0.014				0.008
H-4g			0.260 ^a				0.020 ^a (H-3 + H-5)
			0.258				0.007
			0.229				0.007
							0.006 ^a (H ₂ O)
							0.028
							0.029
H-1fb				0.052 ^a			0.016 ^a (H-1'a)
				0.036			0.010
				0.037			0.011
H-3f					0.310 ^a	0.009 ^a	0.015 ^a (H ₂ O)
					0.270	0.004	0.028
					0.276	0.004	0.035
H-4f						0.241 ^a	
						0.262	
						0.254	

The first set of simulated NOESY volumes corresponds to the all-trans CICADA ensemble-averaged distance matrices while the second set was calculated for the CICADA structure AX155. The motional models were as follows: τ_c values of 0.75 ns, $S_{\text{ang}}^2 = 0.70$ and $\tau_e = 0.1$ ns.

The NOESY volumes calculated for both the all-trans CICADA ensemble-averaged distance matrices ($\langle r^{-3} \rangle$ and $\langle r^{-6} \rangle$) and the AX155 single structure have also been given in Table 6. The signal-to-noise ratios of the experimental crosspeak volumes are low due to the unfavorable tumbling time but, on the whole, the agreements between the theoretical and experimental data sets are very reasonable. A poor fit between the experimental and theoretical $a_{\text{H-1g,H-1g}}$ diagonal volume for the CICADA ensemble-averaged distance matrices is obtained due to less-than-optimum H-1g/H-1fb and H-1g/OH internuclear distances. Cross-relaxation between the methine and α -hydroxyl protons is very efficient (the time-averaged internuclear distances between these spins and the OH protons are generally < 2.5 Å) and an improved estimation of the time-averaged orientation of the hydroxyl groups would undoubtedly be obtained through simulations with explicit solvent. The theoretical NOESY volumes were also calculated for an NMR-derived single structure (AX155) which reproduces both the $^3J_{\text{H-1g,C-2f}}$ and homonuclear coupling constants. A much improved fit for the $a_{\text{H-1g,H-1g}}$ diagonal volume is observed but overall the experimental data and the theoretical NOESY volumes are similar.

From both the vicinal coupling constants between HO-1f and H-1fa (7.3 Hz) and HO-1f and H-1fb (4.9 Hz) and the stronger intensity of the H-1g/H-1fb crosspeak when compared to the H-1g/H-1fa one, the stereospecific assignment of H-1fb to H-1Rf could be inferred.

In conclusion, the conformational preferences of 2-*O*-lauroyl sucrose established with the CICADA algorithm have been corroborated by NMR spectroscopy. Conformational space is more restricted than in the case of sucrose and the time-averaged properties are dominated by a single family of structures. The major conformational change induced by the side chain is the TG orientation of the CH₂-1f primary hydroxyl group which has been demonstrated on the basis of both experimental and theoretical data. Conformational searching has revealed that the potential energies of structures with cis and trans sidechain orientations are very similar which may explain why it has proven so difficult to organize 2-*O*-lauroyl sucrose in the form of single crystals. In the present study, it has not been possible to characterize the dynamics of the lauroyl sidechain through NMR relaxation data as the samples were not stable over a long enough period to collect multifield data. From both the ¹H and ¹³C relaxation data, it appears

that the tumbling of 2-*O*-lauroylsucrose is only slightly anisotropic. A motional model similar to the one recently proposed for sucrose (internal motion of considerable amplitude $S_{\text{ang}}^2 \sim 0.7$) reproduced all the relaxation data.

Acknowledgements

This work was supported by a grant to S.B.E. from the Danish Food Research Centre for Advanced Studies (LMC). S.P. is a staff member of Institut National de la Recherche Agronomique.

References

- [1] W. Kühlbrandt, *Q. Rev. Biophys.*, 25 (1992) 1–49.
- [2] C. Chauvin, K. Bacsko, and D. Plusquellec, *J. Org. Chem.*, 58 (1993) 2291–2295.
- [3] D. Abram, F. Boucher, H. Hamanaka, K. Hiraki, Y. Kito, K. Koyama, R.M. Leblanc, H. Machida, G. Munger, M. Seldon, and M. Tessier, *J. Colloid Int. Sci.*, 128 (1989) 230–235.
- [4] C. Chauvin, Doctoral thesis, University of Rennes (1991) pp. 139–152.
- [5] B. De Foresta, N. Legros, D. Plusquellec, M. Lemaire, and P. Champeil, *Eur. J. Biochem.*, 241 (1996) 343–354.
- [6] F. Ricoul, M. Dubois, A. Vandais, J.P. Noël, T. Zemb, M. Lefeuvre, D. Plusquellec, and O. Diat, *Prog. Colloid Polym. Sci.*, (submitted).
- [7] IUPAC-IUB, Commission on Biochemical Nomenclature, *Arch. Biochem. Biophys.*, Vol. 145, 1971, pp. 405–421.
- [8] P. Ladam, J. Gharbi-Benarous, M. Piotto, M. Delaforge, and J.P. Girault, *Magn. Reson. Chem.*, 32 (1994) 1–7.
- [9] S.B. Engelsen, C. Hervé du Penhoat, and S. Pérez, *J. Phys. Chem.*, 99 (1995) 13334–13351.
- [10] N.L. Allinger, Y.H. Yuh, and J.-H. Lii, *J. Am. Chem. Soc.*, 111 (1989) 8551–8567.
- [11] N.L. Allinger, M. Rahman, and J.-H. Lii, *J. Am. Chem. Soc.*, 112 (1990) 8293–8307.
- [12] A.D. French and M.K. Dowd, *J. Mol. Struct. (Theochem)*, 286 (1993) 183–201.
- [13] A. Imberty, S. Pérez, and J. Koca, *J. Comput. Chem.*, 3 (1995) 296–310.
- [14] S.B. Engelsen, J. Koca, I. Braccini, C. Hervé du Penhoat, and S. Pérez, *Carbohydr. Res.*, 276 (1995) 1–29.
- [15] J. Koca, *J. Mol. Struct. (Theochem)*, 308 (1994) 13–24.
- [16] M. Karplus, *J. Chem. Phys.*, 30 (1959) 11–15.
- [17] C.A.G. Haasnoot, F.A.A.M. de Leeuw, and C. Altona, *Tetrahedron*, 36 (1980) 2783–2792.
- [18] I. Tvaroska, M. Hricovini, and E. Petrakova, *Carbohydr. Res.*, 189 (1989) 359–362.
- [19] K. Bock and J. Ø Duus, *J. Carbohydr. Chem.*, 13 (1994) 513–543.
- [20] N. Bouchemal-Chibani, I. Braccini, C. Derouet, C. Hervé du Penhoat, and V. Michon, *Int. J. Biol. Macromol.*, 17 (1995) 177–182.
- [21] G. Lipari and A. Szabo, *J. Amer. Chem. Soc.*, 104 (1982) 4546–4559.
- [22] A.D. French, L. Schäfer, and S.Q. Newton, *Carbohydr. Res.*, 239 (1993) 51–60.
- [23] F. Casset, A. Imberty, C. Hervé du Penhoat, J. Koca, and S. Pérez, *J. Mol. Struct. (Theochem)*, 395 (1997) 211–224.
- [24] G.M. Brown and H.A. Levy, *Acta Crystallogr., Sect. B.*, 29 (1973) 790–797.
- [25] S.B. Engelsen and S. Pérez, *Carbohydr. Res.*, 292 (1996) 21–38.
- [26] S. Immel and F.W. Lichtenthaler, *Liebigs Annalen*, (1995) 1925–1937.
- [27] F. Casset, T. Hamelryck, R. Loris, J.-R. Brisson, C. Tellier, M.-H. Dao-Chi, L. Wyns, F. Poortmans, S. Pérez, and A. Imberty, *J. Biol. Chem.* 270, (1995) 25619–25628.
- [28] K. Bock and R.U. Lemieux, *Carbohydr. Res.*, 100 (1982) 63–74.
- [29] A.S. Perlin and B. Casu, in G.O. Aspinall (Ed.), *The Polysaccharides*, Vol. 1, Academic Press, New York, 1982, pp. 133–193.
- [30] J.C. Christofides and D.B. Davies, *J. Am. Chem. Soc.*, 105 (1983) 5099–5105.
- [31] J. Reuben, *J. Am. Chem. Soc.*, 106 (1984) 6180–6186.
- [32] R.U. Lemieux and K. Bock, *The Japanese Journal of Antibiotics*, Vol. XXXII, 1979, S-163 to S-177.
- [33] R. Khan, *Adv. Carbohydr. Chem. Biochem.*, 33 (1976) 235–254.
- [34] A.H. Haines, *Adv. Carbohydr. Chem. Biochem.*, 33 (1996) 11–109.
- [35] K. Bacsko, C. Nugier-Chauvin, J. Banoub, P. Thibault, and D. Plusquellec, *Carbohydr. Res.*, 269 (1995) 79–88.
- [36] D.C. McCain and J.L. Markley, *Carbohydr. Res.*, 152 (1986) 73–80.
- [37] D. Pissas, P. Dais, and E. Mikros, *Magn. Reson. Chem.*, 32 (1994) 263–275.
- [38] P.A.J. Gorin, *Adv. Carbohydr. Chem. Biochem.*, 42 (1982) 13–104.
- [39] L. Catoire, V. Michon, L. Monville, A. Hocquet, L. Jullien, J. Canceill, J.M. Lehn, M. Piotto, and C. Hervé du Penhoat, submitted to *Carbohydr. Res.*
- [40] F. Heatley, *Annu. Rep. NMR Spectrosc.*, 17 (1986) 179–230.
- [41] D.E. Woessner, *J. Chem. Phys.*, 37 (1962) 647–654.
- [42] A. Ejchart, J. Dabrowski, and C.-W. von der Lieth, *Magn. Reson. Chem.*, 30 (1992) S105–S114.